UM-TH-94-03
February 1994

PREDICTIONS FOR CONSTRAINED MINIMAL SUPERSYMMETRY WITH BOTTOM-TAU MASS UNIFICATION

Chris Kolda[1], Leszek Roszkowski[2], James D. Wells[3] and G.L. Kane[4],
Randall Physics Laboratory, University of Michigan,
Ann Arbor, MI 48190, USA

Abstract

We examine the Constrained Minimal Supersymmetric Standard Model (CMSSM) with an additional requirement of strict b–τ unification in the region of small $\tan\beta$. We find that the parameter space becomes completely limited below about 1 TeV by physical constraints alone, without a fine-tuning constraint. We study the resulting phenomenological consequences, and point out several ways of falsifying the adopted b–τ unification assumption. We also comment on the effect of a constraint from the non-observation of proton decay.

[1]E-mail: kolda@umich.edu
[2]E-mail: leszekr@umich.edu
[3]E-mail: jwells@umich.edu
[4]E-mail: gkane@umich.edu

1 Introduction

A recent resurgence of strong interest in supersymmetry (SUSY) has led to a number of attempts at exploring the physical spectra and phenomenological consequences associated with the Minimal Supersymmetric Standard Model (MSSM) in the context of Grand Unified Theories (GUTs). This renewed interest is due primarily to the realization that gauge coupling unification within the Standard Model (SM) does not occur at any scale as one would expect from GUTs such as $SU(5)$. On the other hand, within the MSSM such unification is found to be possible. Early studies [1] have been followed by a series of increasingly elaborate, and increasingly precise, analyses which have built complete SUSY spectra consistent with the unification assumption (see [2] and references therein). These studies have mostly used the well-motivated supergravity (SUGRA) assumptions which suggest equating many of the unknown soft SUSY-breaking mass terms at the GUT scale. Within this framework, very complete studies can be done covering the entire range of possible SUSY masses, and specific, testable predictions can be made.

In a previous work [2], we have examined the MSSM under a number of general assumptions about the unification of the gauge couplings and masses, independent of the choice of gauge unification group.[1] Within this context, a number of predictions, bounds, and signals were deduced and studied. A specific choice of GUT model and/or further assumptions or constraints could only serve to sharpen these predictions.

In this letter we consider one further aspect of unification: the apparent unification of the bottom quark and tau lepton Yukawa couplings at the GUT scale, as would be expected in a GUT containing minimal $SU(5)$ Yukawa interactions. Semi-analytic studies completed recently by several groups [2, 3, 4, 5] have found, however, that the MSSM does not in general produce this b–τ mass unification except in small and well-defined regions of the parameter space of m_t and $\tan\beta$. Specifically, it has been realized that, up to GUT-scale threshold corrections, b–τ mass unification can only occur if the top Yukawa coupling is at or near its infrared pseudo-fixed point.

In Ref. [2], we examined the size of the GUT-scale corrections necessary in order to remove the strong constraints on $\tan\beta$ and m_t. We found that $\mathcal{O}(10\%)$ corrections both in the gauge and Yukawa unification were more than adequate for allowing b–τ mass unification over very wide ranges of values for $\tan\beta$ and m_t. Nonetheless, examinations of "typical" GUT threshold corrections [5] have yielded corrections too small to significantly alter the relation between $\tan\beta$ and m_t, so a detailed exploration of the SUSY parameter space indicated by b–τ mass unification seems well-motivated. Our goal is to derive testable experimental consequences of this assumption, and to point out how b–τ mass unification within the MSSM can be falsified in a number of ways. Finally, we will comment on the effects of a constraint from the non-observation of the proton decay.

2 The Pseudo-Fixed Point Solutions

It was recognized several years ago that one of the strengths of the MSSM over the SM was that in the MSSM the b- and τ-Yukawa running couplings meet at roughly the same

[1] We only require that the choice of unification group lead to $\sin^2\theta_{\rm w}(M_X) = \frac{3}{8}$ which also holds in many phenomenologically viable superstring-derived models.

mass scale at which the unification of the gauge couplings takes place [6]. As both the experimental data and the theoretical calculations became more precise, it became clear that gauge coupling unification within the MSSM occurs over the entire range of theoretically acceptable SUSY mass scales. At the same time, however, Yukawa unification within the MSSM is not so trivial. For most choices of input parameters (*e.g.*, $\tan\beta$ and m_t), the τ-Yukawa coupling is as much as $\mathcal{O}(20\%)$ larger than that of the b-quark at the gauge coupling unification scale. And because the slopes of the bottom and tau Yukawas are typically flat at large scales, the Yukawa couplings can "unify" (*i.e.*, cross) at a mass scale many orders of magnitude smaller than the GUT scale, even though their GUT-scale values may differ by only 10–20%.

The exception to this general trend, however, occurs when either *(i)* the top Yukawa coupling, or *(ii)* the b- and τ-Yukawa couplings, are at or very near their infrared pseudo-fixed point values. That pseudo-fixed point value is the value of the Yukawa coupling (at the electroweak scale) which produces a Landau pole precisely at the GUT scale; that is, values of the coupling greater than the fixed point value will become non-perturbative at scales below M_X when run up using its renormalization group equations (RGEs).

The values for the top, bottom, and tau Yukawa couplings corresponding to the pseudo-fixed point can be precisely determined. For the case at hand, one finds [3, 4] that there are two conditions for sitting on or near one of the pseudo-fixed points (that is, for finding b–τ Yukawa unification) either one of which must be satisfied. Either

$$M_t \simeq (200\,\mathrm{GeV})\sin\beta \tag{1}$$

or

$$50 \lesssim \tan\beta \lesssim 70. \tag{2}$$

The first condition corresponds to the top Yukawa pseudo-fixed point, while the second is the bottom-tau Yukawa pseudo-fixed point. Also, because the difference between the top quark pole mass and running ($\overline{\mathrm{MS}}$ or $\overline{\mathrm{DR}}$) mass can be as much as 10 GeV in the region of interest, one must be careful to specify to which top quark mass one is referring. We will use m_q to specify a quark running mass (or a general definition when the choice is irrelevant) and M_q its pole mass.

In Fig. 1 we have shown the region in the $(M_t, \tan\beta)$ plane consistent with b–τ mass unification. The width of the region is due to the 3σ uncertainty in the b-quark mass (using $M_b = 4.9 \pm 0.07\,\mathrm{GeV}$ [7]) and the 1σ uncertainty in $\alpha_s(m_Z)$ ($\alpha_s(m_Z) = 0.120 \pm 0.007$ [8]); in this figure none of the width comes from GUT threshold corrections to the Yukawa unification.

From Fig. 1 it is evident that there are three primary regions of interest in this plane. The first is the region (labelled I) of large $\tan\beta$, over all M_t, where the b- and τ-Yukawa couplings reach their pseudo-fixed points. Some part of this region, corresponding also to large M_t, is of particular interest to those studying $SO(10)$ unification with a minimal Yukawa sector. There one can obtain the GUT-scale prediction $m_b = m_\tau = m_t$, which when renormalized at the electroweak scale yields $\tan\beta \simeq \frac{m_t}{m_b} \simeq 50 \sim 70$. Because of that relation, this region deserves consideration and some studies have been carried out [9, 10, 11]. However, certain difficulties invariably arise in considering the MSSM with very large $\tan\beta$. Three in particular stand out.

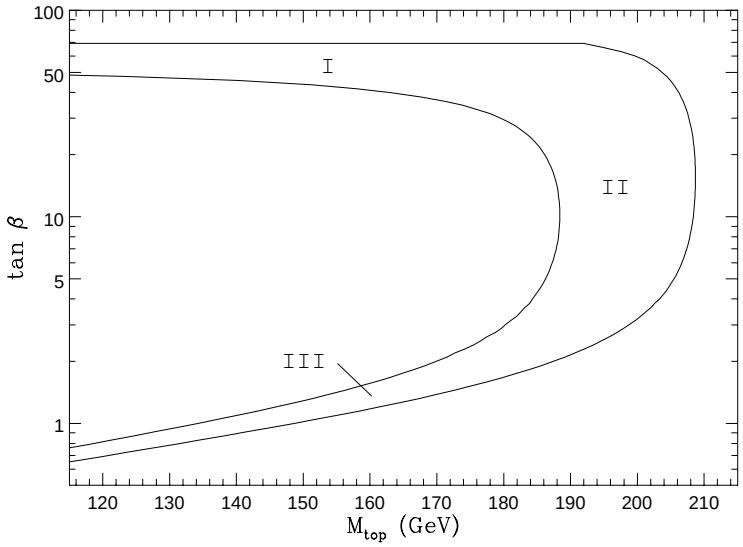

Figure 1: The $(M_t, \tan\beta)$ plane showing the region consistent with b–τ unification. The width of the region is due to the 3σ uncertainty in M_b and the 1σ uncertainty in α_s (see text). The three regions of unification are all visible: (I) $\tan\beta \simeq 50 \sim 70$, (II) $190\,\text{GeV} \lesssim M_t \lesssim 210\,\text{GeV}$, and (III) $\tan\beta \simeq 1$.

First, it has been argued that within the MSSM (with two Higgs doublets) large $\tan\beta$ is unnatural [12]. Specifically, one finds that large hierarchies, only some of which can be protected by additional imposed symmetries, arise among the mass parameters of the Higgs potential. Second, one has particular difficulty with the 1-loop corrections to the b-quark mass, which are proportional to $\tan\beta$ and can easily be of $\mathcal{O}(50\%)$ unless new symmetries are imposed in order to control them [10]. This issue has been more recently investigated in Ref. [11] in the context of an $SO(10)$ GUT model and it has been argued that requiring dynamical electroweak symmetry breaking makes those corrections well defined though generally unsuppressed. Finally, models with large $\tan\beta$ tend to produce very small branching ratios for the FCNC process $b \to s\gamma$ due to their suppressed charged Higgs contributions, perhaps inconsistent with recent CLEO data. Therefore, we choose to put off any further consideration of this region for now.

The second region (labelled II in Fig. 1) leading to b–τ mass unification is found at large M_t between about 190 and 210 GeV for almost all values of $\tan\beta$ (between about 2 and 60). This region of parameter space is strongly disfavored by the 2σ LEP limit $m_t \lesssim 180\,\text{GeV}$ for $m_{h^0} < 120\,\text{GeV}$ [13]. Further, if FNAL does see top quark events, one could exclude top quark masses in this region due to the small cross section expected for such large m_t. Therefore, we will not consider this region in the present study.

The third and final region (labelled III in Fig. 1) is at low $\tan\beta$, with $M_t \lesssim 190\,\text{GeV}$, where there is almost a one-to-one correspondence between $\tan\beta$ and M_t. This range is perhaps of more immediate interest since it corresponds to the top mass range to be covered by the Tevatron. And, having disfavored the previous two regions, we are led to consider in

detail this region of $\tan\beta$ near one, for $155\,\mathrm{GeV} \leq M_t \leq 185\,\mathrm{GeV}$. As we will show below, this scenario leads to very specific and falsifiable predictions which could rule it out.

One should remark on the size of the radiative corrections to the b-quark mass in the low $\tan\beta$ regime. We find for all solutions in this third region that the (leading) gluino-induced corrections to the bottom quark mass are always small, $\delta m_b/m_b \lesssim 2\%$; the higgsino-induced corrections are approximately four times smaller still. These corrections are far too small to alter our results. We also find that the sizes of these corrections depend only very weakly on the SUSY mass parameters m_0, $m_{1/2}$, and μ in fully consistent solutions (see following section), and so remain small even at large SUSY mass scales.

3 The Constrained Minimal Supersymmetric Standard Model (CMSSM)

In Ref. [2], we described the construction of what we termed the Constrained MSSM (or CMSSM), built by relating the MSSM soft-breaking terms through the minimal SUGRA assumptions and then constraining these solutions as summarized below. Here we briefly summarize the basic points of that construction.

For each choice of M_t, m_0, $m_{1/2}$, A_0, and $\mathrm{sgn}\,\mu_0$ ($\tan\beta$ is now determined through the requirement of b–τ unification as described earlier) we find a solution in the CMSSM; each solution is a complete set of values for α_s and the masses of the Higgs bosons and all the superpartners. (The exact procedure for building such complete solutions is summarized in Ref. [2].) If the Higgs potential at the electroweak scale does not admit electroweak symmetry breaking (EWSB) consistent with the SM, that choice of input parameters is discarded. Further constraints are then applied.

Besides requiring that EWSB occur, we demand that all physical mass-squares remain positive. We demand that all solutions be unobservable by current direct experimental searches, including the requirement that the solutions provide a $\mathrm{BR}(b \to s\gamma)$ consistent with CLEO data. Furthermore, we calculate the relic density of the lightest SUSY particle (LSP), demanding only that the LSP be neutral, and, from limits on the age of the universe of 10 billion years, we demand that $\Omega_{LSP}h_0^2 < 1$. Those solutions which finally remain after all these cuts comprise the allowed parameter space of the CMSSM.

4 Results

We have examined solutions for three representative top quark (pole) masses of M_t =155, 170, and 185 GeV in order to study the range that seems to be indicated by the LEP analysis and early CDF results. In building the parameter space of solutions, we have varied m_0 and $m_{1/2}$ from 20 GeV to the TeV scale logarithmically; no upper bound is set by hand on m_0 or $m_{1/2}$, their upper bounds coming from the constraints on the solutions which define the CMSSM. The lower bound of m_0 was not taken to zero, but values in the lower region ($m_0 \simeq \mathcal{O}(20\,\mathrm{GeV})$) are for all purposes phenomenologically identical to each other as well as to No-Scale models, since experimental bounds force $m_{1/2} \gtrsim 80\,\mathrm{GeV}$. The value of A_0 was restricted to the range $-2.5 \leq A_0/m_0 \leq 2.5$ in order to avoid possible color-breaking minima of the full scalar potential. The final free parameter, $\mathrm{sgn}\,\mu_0$, was allowed to take

both possible values.

4.1 Allowed Parameter Space and Mass Spectra

One of the remarkable consequences of considering this low $\tan\beta$ limit with a complete analysis is the existence of upper bounds on the mass parameters of the MSSM *without resorting to an imposed arbitrary fine-tuning condition*. In particular the combination of various mass bounds from direct searches, the age of the universe constraint, and the requirement that the LSP be electrically neutral combine to put strict upper (and lower) bounds on m_0 and $m_{1/2}$, and therefore on the mass spectrum of the MSSM. These bounds are entirely due to the physical constraints of the CMSSM. As we pointed out previously [2], for small $\tan\beta \lesssim 2$ and/or large $m_t \gtrsim 170\,\mathrm{GeV}$, the parameters $m_{1/2}$ and m_0 (and therefore the whole SUSY spectrum) are completely constrained from above in the $\mathcal{O}(1\,\mathrm{TeV})$ range. The case considered here falls into that category. These absolute upper bounds are m_t-dependent and are usually somewhat weaker than those imposed by simply requiring all SUSY masses below about 1 TeV, or than those which the fine-tuning constraint we used in Ref. [2] would have permitted. For this reason, in examining some phenomenological applications of the solutions in the CMSSM, we will place an additional fine-tuning constraint. We do so in order to ensure that phenomenological results of this study are "realistic"; that is, although consistent solutions may exist with large SUSY mass scales, we wish to exclude these from phenomenological consideration on the basis that they reintroduce too much fine-tuning into the physics. (Our precise definition of fine-tuning is discussed in Ref. [2]. We note that the definition that we use diverges at $\tan\beta = 1$; the values of $\tan\beta$ that we consider here are far enough from unity so that this effect is not significant, and becomes irrelevant as $\tan\beta$ increases with increasing m_t.)

In Fig. 2 we have shown the allowed range of parameter space in the $(m_{1/2}, m_0)$ plane for $M_t = 155$ (Fig. 2a), 170 (Fig. 2b), and 185 GeV (Fig. 2c) without fine-tuning constraints. All three graphs exhibit many similarities which are general features of the CMSSM for all $\tan\beta$ [2]. In both cases the region of large $m_{1/2} \gg m_0$ is excluded by demanding a neutral LSP. This uniquely selects the lightest neutralino $\chi \equiv \chi_1^0$ (mostly a bino-like state) for which we calculate the relic abundance. Then we find that large m_0 are excluded by requiring $\Omega_\chi h_0^2 < 1$.

For the $M_t = 155\,\mathrm{GeV}$ case, we find that Yukawa unification allows $\tan\beta$ to take on values only in the range $1.1 \lesssim \tan\beta \lesssim 1.4$. This, coupled with the requirements of the CMSSM, restricts $80\,\mathrm{GeV} \lesssim m_{1/2} \lesssim 940\,\mathrm{GeV}$ and $m_0 \lesssim 350\,\mathrm{GeV}$. When we apply the fine-tuning constraint $f \leq 50$, we find the approximate bound shown as a solid line in Fig. 2a. For this subset of solutions, we find new upper bounds on the parameters of the model. In particular, the fine-tuning constraint yields $\tan\beta \lesssim 1.2$, $m_{1/2} \lesssim 180\,\mathrm{GeV}$ and $m_0 \lesssim 210\,\mathrm{GeV}$. Notice also the strong lower bounds placed on the parameter space. This bound comes from two sources: for $\mu > 0$, solutions with small $m_{1/2}$,m_0 are ruled out by the Higgs mass bound; for $\mu < 0$, it is the $\widetilde{t}_1$ mass bound that rules out the same approximate region. This effect is strongly diminished with increasing $\tan\beta$ (and therefore M_t).

The $M_t = 185\,\mathrm{GeV}$ case in Fig. 2c exhibits one additional interesting feature. For a relatively narrow range of $m_{1/2} \simeq 100\,\mathrm{GeV}$ solutions with much larger m_0 are allowed. The source of this behavior is the Z-pole enhanced neutralino pair annihilation into a pair

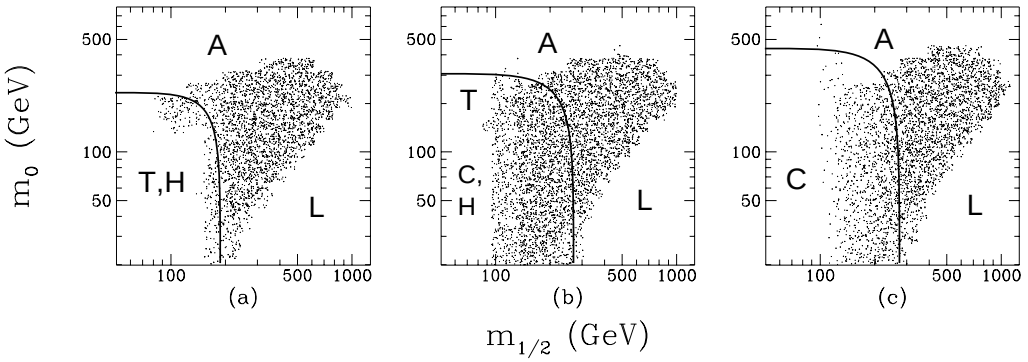

Figure 2: The regions of the $(m_{1/2}, m_0)$ plane consistent with low $\tan\beta$ b–τ mass unification, given all the constraints of the CMSSM. For (a) $M_t = 155\,\mathrm{GeV}$, (b) $M_t = 170\,\mathrm{GeV}$ and (c) $M_t = 185\,\mathrm{GeV}$. Each dot represents one solution belonging to the CMSSM. Because m_0 and $m_{1/2}$ are discrete inputs in this approach, the points have been "smeared" to show variations in density. The regions with no solutions are labelled as to which constraints forbid solutions there: age of universe bound (**A**), neutral LSP requirement (**L**), non-tachyonic stop (**T**); Higgs mass bound (**H**), and chargino mass bound (**C**). The solid curves in each figure are the approximate cutoffs dictated by our choice of fine-tuning constraint.

of ordinary fermions. (For $m_{1/2} \simeq 100\,\mathrm{GeV}$, $m_\chi \simeq 0.45\, m_{1/2} \simeq m_Z/2$.) This exchange vanishes in the limit $\tan\beta = 1$ and is therefore negligible in Fig. 2a where $\tan\beta \lesssim 1.4$. For $M_t = 185\,\mathrm{GeV}$, we find $1.8 \lesssim \tan\beta \lesssim 3.1$ and the effect of the Z-exchange becomes important. Our analysis provides an overall envelope of $100\,\mathrm{GeV} \lesssim m_{1/2} \lesssim 1.1\,\mathrm{TeV}$ and $m_0 \lesssim 600\,\mathrm{GeV}$. Once again the fine-tuning constraint tends to lower the upper bounds of the various model parameters. In particular, we find $\tan\beta \lesssim 2.4$, $m_{1/2} \lesssim 290\,\mathrm{GeV}$ and $m_0 \lesssim 420\,\mathrm{GeV}$ after applying the fine-tuning constraint. The corresponding fine-tuning bound is shown as a solid line in Fig. 2c.

The intermediate case for $M_t = 170\,\mathrm{GeV}$ in Fig. 2b does demonstrate some hint of the Z-pole effect found at the larger $\tan\beta$ associated with $M_t = 185\,\mathrm{GeV}$. Here we find $1.4 \lesssim \tan\beta \lesssim 1.9$, $90\,\mathrm{GeV} \lesssim m_{1/2} \lesssim 940\,\mathrm{GeV}$, and $m_0 \lesssim 500\,\mathrm{GeV}$ without a fine-tuning constraint. Upper bounds with the fine-tuning constraint are modified to be $\tan\beta \lesssim 1.5$, $m_{1/2} \lesssim 260\,\mathrm{GeV}$ and $m_0 \lesssim 300\,\mathrm{GeV}$.

It is worth noting that the region $m_0 \gg m_{1/2} \simeq m_Z$ (and small $\tan\beta$) is favored by the non-observation of proton decay in $SU(5)$-based GUTs with minimal Higgs sector [14]. In this case the neutralino relic abundance is reduced by the Z- and h^0-pole effects. In this region the LSP still remains mostly bino-like, although with somewhat smaller bino component ($\gtrsim 90\%$). However, predictions for proton decay can be suppressed with more complicated Higgs sectors (see, *e.g.*, Ref. [15]) and, since we do not assume any specific GUT model here, we will also not use this constraint to limit the parameter space of the CMSSM. We also note that our numerical routine for the relic abundance is not designed to properly calculate $\Omega_\chi h_0^2$ in the vicinity of a pole (that is, within about 10 GeV of the pole) and therefore the values of $\Omega_\chi h_0^2$ in this regions are only indicative.

One should note for all bounds throughout this study that the exact values depend on

Mass Limits (GeV)	$M_t = 155\,\text{GeV}$			170 GeV			185 GeV		
	lower	upper	FT	lower	upper	FT	lower	upper	FT
$m_{1/2}$	80	940	180	90	940	260	100	1060	290
m_0	0	350	210	0	500	300	0	600	420
$\lvert\mu(m_Z)\rvert$	520	1800	660	250	1470	560	210	1390	520
M_2	65	780	150	70	780	210	80	880	240
h^0	60	105	81	60	124	99	75	149	118
A^0	730	2550	925	330	2040	770	260	1910	710
$\widetilde{t}_1$	38	1340	215	38	1400	470	115	1550	510
$\widetilde{\tau}_1$	65	420	210	50	500	300	55	600	420
$\widetilde{l}_L$	115	670	215	65	710	310	70	780	430
$\widetilde{q}$	235	1740	425	245	1870	590	255	2100	670
$\widetilde{g}$	215	2030	450	240	2040	630	270	2300	710
χ =LSP	35	410	70	25	410	110	25	465	125
$\chi_1^\pm \simeq \chi_2^0$	75	770	135	48	780	220	48	875	245
$\tan\beta$	1.1	1.4	1.2	1.4	1.9	1.5	1.8	3.1	2.4
$\alpha_s(m_Z)$	0.117	0.125	0.121†	0.122	0.129	0.124†	0.124	0.133	0.124†

† Lower bound with FT constraint.

Table 1: The bounds of the masses and parameters of the MSSM under the constraint of low $\tan\beta$ Yukawa unification for $M_t = 155$, 170, and 185 GeV. For each top quark mass the lower bound (labelled *lower*), the absolute upper bound with no fine-tuning constraint (*upper*) and the upper bound with the fine-tuning constraint (*FT*) are shown. All masses are in GeV. The general masses $\widetilde{q}$ and $\widetilde{l}_L$ represent the bounds on all squarks and LH-sleptons excluding the third generation. The bounds on all first and second generation RH-sleptons are essentially those of the $\widetilde{\tau}_1$ for low $\tan\beta$. Note that there is sensitivity to the grid of values for $(m_0, m_{1/2}, A_0)$ that we have chosen, and therefore some uncertainty in the exact bounds.

our numerical sampling of the original input parameter space and so should be considered with appropriate errors. In particular, upper (lower) bounds on $m_{1/2}$ could be modified upwards (downwards) by as much as 12% with a smaller sampling grid; bounds on m_0 could likewise be increased (decreased) by as much as 20%.

Because such strict bounds exist for these cases (with and without fine-tuning), we can place bounds on the CMSSM mass spectra. In Table 1 the numerical bounds on a variety of important quantities are shown for all three top masses, with and without the fine-tuning constraint.

It is significant that much of the region of low $m_{1/2}$ for the $M_t = 155\,\text{GeV}$ case has been excluded on the basis of the non-discovery of the Higgs boson in direct searches. For all solutions in the superunified MSSM, the lightest Higgs scalar (h^0) has essentially identical properties to those of its SM counterpart; that is $\sin^2(\beta - \alpha) \approx 1$ always. Therefore mass bounds on the SM Higgs apply equally well to the h^0. (We conservatively require $m_{h^0} > 60\,\text{GeV}$.) However, h^0 receives large one-loop radiative corrections which can increase its mass by $\mathcal{O}(m_Z)$. Therefore, limits on the solution space based on Higgs non-observation must include the full one-loop radiative corrections, which in turn requires a full calculation of the SUSY mass spectra, particularly the mass eigenstates of the top squarks.

Because the top mass dependence of these radiative corrections is so strong, one can clearly understand why the lower bound on $m_{1/2}$ due to the Higgs mass decreases with

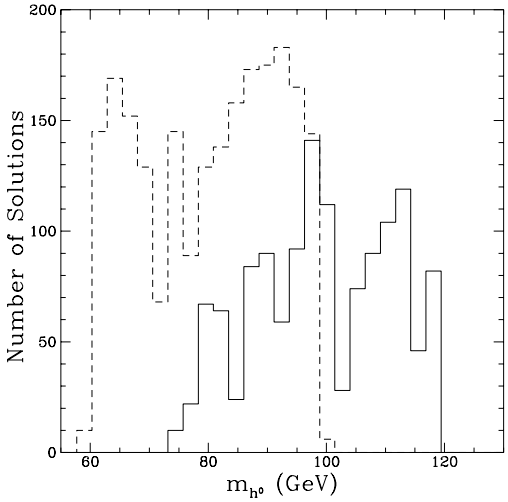

Figure 3: The number of solutions with a given m_{h^0} versus the value of m_{h^0}, for $M_t = 170\,\mathrm{GeV}$ (dashed) and 185 GeV (solid). Only the solutions with small fine-tuning are plotted.

increasing m_t; for larger m_t, one gets larger m_{h^0} from radiative corrections, so the experimental bound on m_{h^0} rules out less of parameter space. In Fig. 3 we demonstrate this behavior by plotting the number of solutions leading to a given m_{h^0} versus m_{h^0}, both for $M_t = 170\,\mathrm{GeV}$ (dashed) and 185 GeV (solid), subject to our fine-tuning constraint.

There are also upper bounds on m_{h^0}, and several groups have recently examined these bounds within this approach [13, 16, 17]. However, because in the $\tan\beta \to 1$ limit $m_{h^0}^2 \to 0$ at tree-level, these bounds are highly dependent on the size of the radiative corrections to $m_{h^0}^2$. And because these corrections increase quartically with m_t and logarithmically with the SUSY masses, their size is highly dependent on one's assumptions about how to cut off the allowed MSSM parameter space, that is, how one defines what "too much fine-tuning" means.

For $M_t = 155$, 170, and 185 GeV, we find m_{h^0} to be less than 81, 99, and 118 GeV respectively, with the fine-tuning condition $f < 50$ imposed. Without this condition, the upper bounds increase, as the effective SUSY mass scale is somewhat increased (compare Table 1). Though we believe that it is the first set of bounds that should be taken as more indicative of our expectations since they more fully contain theoretical prejudices which apply to SUSY, one should bear in mind the strong dependence of these bounds on the choice of fine-tuning condition. This caveat, however, does not apply to the maximum values as given in Table 1, where no fine-tuning condition at all was used to bound the parameter space. One should also note that calculations of the two-loop corrections to m_{h^0} show a net decrease of m_{h^0} below its one-loop value [18], and therefore will not disrupt our bounds.

Detection of the other Higgs bosons (H^0, A^0, and $H^\pm$) cannot be accomplished at LEP II nor at the proposed NLC500 [19]. We find for $155\,\mathrm{GeV} \le M_t \le 185\,\mathrm{GeV}$ that $m_{H^0} \simeq m_{A^0} \simeq m_{H^\pm} \ge 260\,\mathrm{GeV}$, outside the range of either machine. We believe that the detection of the heavier Higgs scalar H^0 might be possible at the LHC somewhat beyond

the asserted region $m_{H^0} \lesssim 2M_t$ [20]. However, all solutions (with small fine-tuning) do have at least one SUSY particle that is detectable at the LHC in addition to the h^0, even if the heavy Higgs bosons are not.

Can LEP II find any sparticles? We find that under the assumption of low $\tan\beta$ b–τ unification, detection of states other than the lightest Higgs may be possible, but for a few solutions only. Searches for light SUSY particles should concentrate on the lighter stop ($\widetilde{t}_1$), the lighter stau ($\widetilde{\tau}_1$), the lighter chargino ($\chi_1^\pm$) and the second lightest neutralino (χ_2^0, where $m_{\chi_2^0} \simeq m_{\chi_1^\pm}$). Within the range of M_t considered, we find solutions with masses for these particles all the way down to their current experimental limits. In particular, for such light stops there is a large mixing of the right-handed and left-handed interaction eigenstates, so the simple approximation that $\widetilde{t}_1 \simeq \widetilde{t}_R$ does not hold. Further studies of the detectability of the MSSM under similar constraints and assumptions have been done in Ref. [17, 21].

We finally note that the resulting ranges of $m_{\widetilde{g}}$ and scalar quark masses are largely above the reach of the Tevatron. Thus finding any of those particles well below the ranges indicated in Table 1 would rule out the b–τ unification if $\tan\beta$ is close to one.

4.2 BR$(b \to s\gamma)$

In the general superunified MSSM where Yukawa unification has not been required, the recent CLEO bounds on BR$(b \to s\gamma)$ have the ability to rule out certain regions of parameter space and indicate a future ability to further constrain or discover SUSY through more precise measurements of BR$(b \to s\gamma)$ [2]. However, one finds in the region of low $\tan\beta$ Yukawa unification that almost all solutions consistent with all other requirements of the CMSSM naturally fall within the bounds of the CLEO data, and in particular, no solutions provide larger branching ratios than are allowed by the data. (We follow Ref. [22] for our calculations of the branching ratio.) But as the following analysis emphasizes, this is not in general due simply to the decoupling of the SUSY contributions; in fact, for solutions with low fine-tuning, the SUSY and SM contributions are often comparable in size.

Nonetheless, what is particularly noteworthy in the low $\tan\beta$ and small fine-tuning limit is that the branching ratio is highly dependent on the sign of μ. In Fig. 4 we have histogrammed our calculated BR$(b \to s\gamma)$ for $M_t = 170$ and 185 GeV solutions with small fine-tuning (we comment on relaxing the fine-tuning condition below). The central peaked region falls approximately at the SM prediction of the branching ratio, with larger M_t moving the peak (and the SM prediction) to larger values. Note however that the histogram yields two separate, non-overlapping regions. In both cases, the region of higher branching ratio is occupied only with solutions of $\mu > 0$. Likewise the region of lower branching ratio is occupied only with solutions of $\mu < 0$. Presuming that both theoretical and experimental uncertainties to $b \to s\gamma$ ever become small enough, one may then have a method by which to differentiate the sign of μ through this process.

Why the two separate regions? Of the non-SM contributions to the $b \to s\gamma$ amplitude, the dominant contribution in this region of parameter space tends to come from the $\chi_1^\pm$–$\widetilde{t}_1$ loop, with sign opposite to that of the SM $W^\pm$–t contribution. For all acceptable solutions of the CMSSM, one gets a lighter chargino that is almost pure $\widetilde{W}^\pm$ and so only has couplings to $\widetilde{t}_L$. Without mixing of the $\widetilde{t}$'s it is the $\widetilde{t}_R$ that invariably comes out to be the lightest squark, which leads to a very small $\chi_1^\pm$–$\widetilde{t}_1$ contribution

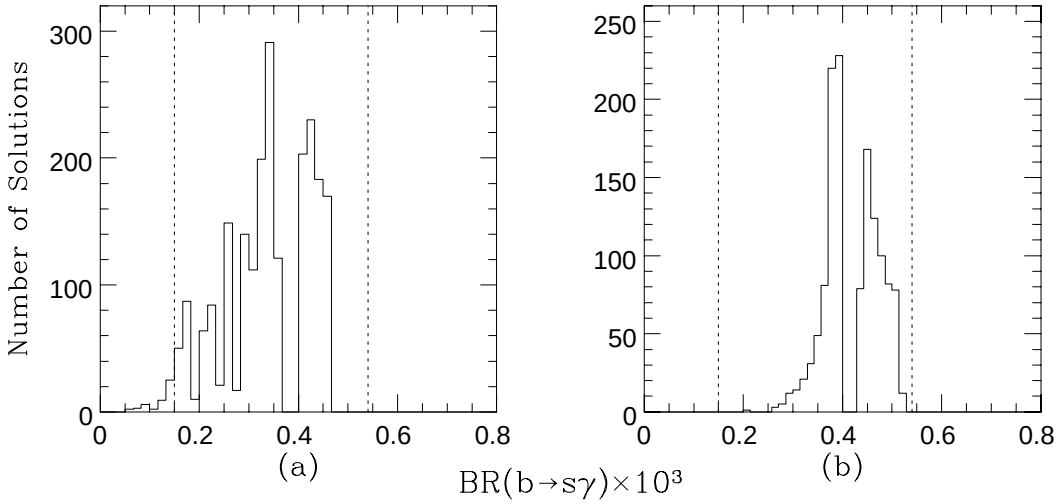

Figure 4: Histogram of BR($b \to s\gamma$) for (a) $M_t = 170\,\mathrm{GeV}$ and (b) $M_t = 185\,\mathrm{GeV}$, for solutions corresponding to low fine-tuning.

Now it is well known that the $\widetilde{t}_L$ and $\widetilde{t}_R$ can have large mixings proportional to $m_t^2(A_t + \mu/\tan\beta)^2$. For small mixings the lighter stop ($\widetilde{t}_1$) is almost pure $\widetilde{t}_R$; as the mixing increases $\widetilde{t}_1$ gains a larger $\widetilde{t}_L$ component and so the $\chi_1^\pm$–$\widetilde{t}_1$ contribution becomes sizeable. For solutions in which m_0 is not too much larger than $m_{1/2}$, one finds that A_t is driven negative at the electroweak scale regardless of its magnitude and sign at the unification scale. Therefore, if μ is also negative, large $\widetilde{t}_L$–$\widetilde{t}_R$ mixings result and $\widetilde{t}_1$ has a sizeable $\widetilde{t}_L$ component; if $\mu > 0$, the A_t and μ contributions to the mixing tend to cancel, forcing the $\widetilde{t}_L$ component of $\widetilde{t}_1$ to be very small.

In the $\mu > 0$ case, then, the $\chi_1^\pm$–$\widetilde{t}_1$ coupling will be very small, allowing the SM contribution to easily dominate. In the $\mu < 0$ case, however, the coupling will be sizeable, cancelling much or all of the SM contribution. Therefore, the $\mu < 0$ case will give much smaller branching ratios than one would get from the $\mu > 0$ case, with the two regions separated near the SM prediction.

What happens as we allow larger $\tan\beta$ or larger fine-tuning? Since the $\widetilde{t}_L$–$\widetilde{t}_R$ mixing goes as $(A_t + \mu/\tan\beta)^2$, it is clear that as $\tan\beta$ increases, A_t will come to dominate the mixing and the results will be relatively independent of $\mathrm{sgn}\,\mu_0$. Similarly, the dependence on $\mathrm{sgn}\,\mu_0$ disappears for solutions corresponding to larger fine-tuning because in this case μ typically becomes large and its contribution dominates over that of A_t, producing mixings proportional only to $(m_t\mu)^2$. However, as expected, for solutions corresponding to large fine-tuning, and therefore large masses in the loops, the supersymmetric contributions go to zero, leaving only the SM contribution and thus no $\mathrm{sgn}\,\mu_0$ dependence anyway.

4.3 The μ-parameter

Of particular interest is the Higgs/higgsino mass parameter μ which does not break SUSY and therefore could in principle take values much larger than the soft SUSY-breaking param-

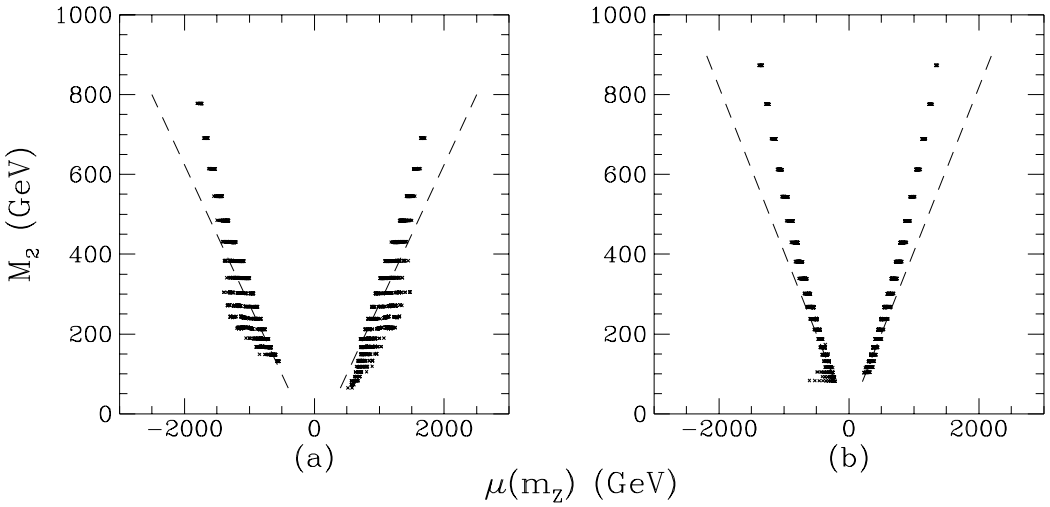

Figure 5: Scatter plot of M_2 versus $\mu(m_Z)$ for (a) $M_t = 155\,\mathrm{GeV}$ and (b) $M_t = 185\,\mathrm{GeV}$ for all solutions in the CMSSM without a fine-tuning constraint. Notice the "$m_0 \gg m_{1/2}$" points present in (b) allowed because those solutions have LSP's falling in the pole of the Z-channel annihilations. The tree level calculation of the μ-M_2 correlation is also shown (dashed line).

eters. In this approach, however, its size is determined through the condition of electroweak symmetry breaking and comes out to be of the same order of magnitude as $m_{1/2}$ and m_0, as has been discussed in detail in Ref. [2] and many other places. Further potentially strong correlations can be derived by imposing additional constraints or assumptions, like the b–τ unification discussed here.

Working in the top Yukawa pseudo-fixed point limit, the authors of Ref. [23] found semi-analytic expressions indicating a strong correlation between μ and $m_{1/2}$ in the region of Yukawa unification. Though their results were only at tree level and so did not contain contributions from the one-loop effective potential, they are easily extended to include the leading correction from the $\widetilde{t}$ sector. We find that for $m_{1/2} > m_0, m_Z$:

$$\mu^2 \simeq m_{1/2}^2 \, \frac{0.5 + 3.5\tan^2\beta}{\tan^2\beta - 1} - \frac{15\alpha_2}{2\pi}\left(\frac{m_t^2}{m_W^2}\right)\left[\log\left(\frac{5m_{1/2}^2}{m_Z^2}\right) - 1\right]. \tag{3}$$

The first term on the right in Eq. (3) is the tree level contribution only [23], while the second term represents the one-loop leading correction.

We illustrate the behavior of μ as a function of M_2 ($M_2 \simeq 0.8\, m_{1/2}$) in Fig. 5 for our solutions with (a) $M_t = 155\,\mathrm{GeV}$ and (b) $M_t = 185\,\mathrm{GeV}$. One can compare this to Fig. 31 of Ref. [2] where the (μ, M_2) plane for general solutions in the CMSSM was displayed. There one does not see evidence for the strong correlation between μ and M_2 (or $m_{1/2}$) that one finds in the pseudo-fixed point limit. We have also plotted in Fig. 5 a dashed line corresponding to the tree level calculation of μ as given by the first term in Eq. (3).

From Fig. 5 one sees that the tree level expression for the μ–$m_{1/2}$ correlation describes our solutions well until $M_2 \gtrsim 400\,\mathrm{GeV}$, where the slope rises due to the one-loop corrections. The one-loop effects are large enough so that the tree level calculation for μ at $m_{1/2} \simeq 1\,\mathrm{TeV}$

is $\mathcal{O}(50\%)$ larger than the actual one-loop value.

One should note, however, that there is an ambiguity in the choice of scale at which one renormalizes the SUSY masses versus the scale at which one minimizes the potential, leading to uncertainties in the one-loop contributions that can be large. The problem stems from the fact that we minimize the potential at $Q = m_Z$, while the SUSY masses are renormalized at their thresholds. This leads to corrections of the one-loop potential that, though of two-loop order, can become significant [13, 24]. Nonetheless, because the solutions with large one-loop contributions are disfavored by fine-tuning arguments, one can safely ignore this question.

The only significant deviation from Eq. (3) occurs in Fig. 5b for some points at very low $m_{1/2}$. These points correspond to the $m_0 \gg m_{1/2}$ points in Fig. 2 where the relic density was suppressed due to the presence of the Z- and h^0-poles. These points can be missed in semi-analytic approaches without calculating the neutralino relic density. It is also this region which SUSY–$SU(5)$ proton lifetime calculations like those of Ref. [14] select. For these points we are far from the limit in which Eq. (3) holds and one finds instead for $m_0 \gg m_{1/2}, m_Z$ another tree-level correlation between μ and m_0 [23] which fits our solutions well (the effects of the one-loop effective potential here are very small):

$$\mu^2 \simeq m_0^2 \, \frac{1 + 0.5 \tan^2 \beta}{\tan^2 \beta - 1}. \tag{4}$$

Finally, one also sees from Fig. 5 that one can put absolute upper and lower bounds on $|\mu|$ within this framework, without regard to M_2. We have included these M_t-dependent bounds in Table 1 and Fig. 5.

4.4 Neutralino Relic Abundance and Dark Matter

We have already emphasized the crucial role played by cosmological constraints in deriving upper bounds of $\mathcal{O}(1\,\text{TeV})$ on the supersymmetric mass parameters, *without* having to impose a somewhat arbitrary constraint of fine-tuning. The main ingredients that lead to such upper bounds in the CMSSM are: *(i)* the lightest neutralino χ comes out to be the only possible LSP which is neutral; and *(ii)* it turns out to be predominantly bino-like.

Even after rejecting solutions with charged LSPs as dark matter (DM) candidates (in our case it is $\widetilde{\tau}_1$ in the region $m_{1/2} \gg m_0$), the sneutrino could still have come out to be the (neutral) LSP. However, just as in the more general case without Yukawa coupling unification [2], we never find that to be the case after we apply experimental limits. Furthermore, the neutralino LSP comes out to be almost pure bino ($p_{\widetilde{B}} \gtrsim 95\%$ except for the region of $m_0 \gg m_{1/2}$ where $p_{\widetilde{B}} \gtrsim 90\%$) because of the radiative EWSB requirement which effectively leads to $|\mu| \gtrsim M_2$ (see Fig. 5).

Finally, it should be appreciated (even if it has been known for some time) that a neutralino relic abundance $\Omega_\chi h_0^2$ close to unity corresponds to sfermion masses in the range of a few hundred GeV, which is a natural mass scale in the MSSM with softly broken SUSY and radiative EWSB. This fact makes the neutralino an excellent candidate for the dark matter in the universe.

Since in this approach all the masses and couplings are determined in terms of just a few basic parameters, we can also reliably calculate $\Omega_\chi h_0^2$ as a function of those same input

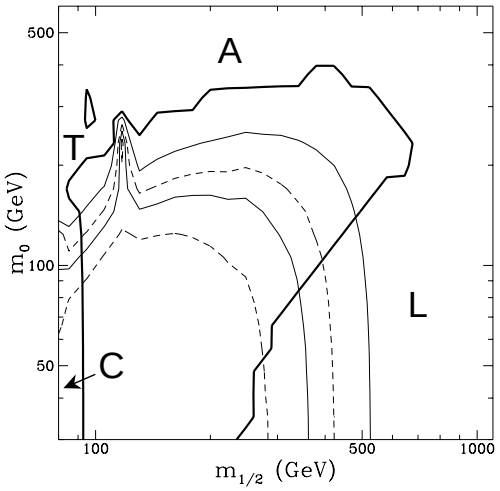

Figure 6: The regions of the $(m_{1/2}, m_0)$ plane consistent with low $\tan\beta$ b–τ mass unification, given all the constraints of the CMSSM, for $M_t = 170\,\mathrm{GeV}$, $A_0/m_0 = 0$ and $\mu < 0$. Solutions outside the thick solid lines are excluded: on the left (small $m_{1/2}$) by the chargino mass bound (**C**) $m_{\chi^\pm} > 47\,\mathrm{GeV}$ and by tachyonic $\widetilde{t}$'s (**T**); on the right (large $m_{1/2} \gg m_0$) by charged LSP (**L**); and from above by the age of the universe, *i.e.* $\Omega_\chi h_0^2 \leq 1$ (**A**). We also indicate the sub-regions selected by either the hypothesis of cold dark matter ($0.25 \lesssim \Omega_\chi h_0^2 \lesssim 0.5$, between thin solid lines) or the one of mixed dark matter ($0.16 \lesssim \Omega_\chi h_0^2 \lesssim 0.33$, between thin dashed lines).

parameters. We include all the final states in calculating the neutralino pair annihilation even though the dominant contribution in most of the parameter space (away from the poles) comes from the exchange of the (lightest) sfermions.

We reject those solutions for which $\Omega_\chi h_0^2 > 1$ as corresponding to the universe being too young (less than about 10 billion years). This requirement alone appears to be extremely powerful, excluding values of $m_{1/2}$ and m_0 bigger than roughly 1 TeV and thus making *low-energy* supersymmetry a *unique* outcome of the simplest SUSY grand-unification assumptions. This is illustrated in Figs. 2 and 6.

Furthermore, there is growing evidence for the existence of dark matter in the universe. While its amount and nature remain unclear, one of the most favored scenarios has been a flat universe ($\Omega = 1$) with most of its matter (about 95%) contributed by DM. In one popular scenario the neutralino would be the predominant component of such (cold) DM in which case its relic abundance would be expected to be

$$0.25 \lesssim \Omega_\chi h_0^2 \lesssim 0.5. \qquad \text{(CDM)} \tag{5}$$

More recently (after COBE), a mixed CDM+HDM picture (MDM) has gained more attention as apparently fitting the astrophysical data better than the pure CDM model. In the mixed scenario one assumes about 30% HDM (like light neutrinos with $m_\nu \simeq 6\,\mathrm{eV}$) and about 65% CDM (bino-like neutralino), with baryons contributing the remaining 5% of the DM. In this case the favored range for $\Omega_\chi h_0^2$ is approximately given by

$$0.16 \lesssim \Omega_\chi h_0^2 \lesssim 0.33. \qquad \text{(MDM)} \tag{6}$$

Mass Limits (GeV)	MDM		CDM		MDM/CDM + FT
	lower	upper	lower	upper	
$m_{1/2}$	90	520	90	660	230
m_0	55	245	85	245	245
$\|\mu(m_Z)\|$	270	940	280	1120	560
M_2	80	430	80	545	190
h^0	62	113	62	118	98
A^0	370	1270	380	1530	770
$\widetilde{t}_1$	95	830	82	1020	430
$\widetilde{\tau}_1$	94	250	110	310	250
$\widetilde{l}_L$	105	380	120	480	260
$\widetilde{q}$	255	1110	265	1350	550
$\widetilde{g}$	250	1200	250	1480	570
χ =LSP	25	225	25	290	100
$\chi_1^\pm \simeq \chi_2^0$	48	435	48	550	200
$\tan\beta$	1.4	1.7	1.4	1.8	1.5
$\alpha_s(m_Z)$	0.123	0.128	0.123	0.128	$0.125^\dagger$

† Lower bound with FT constraint.

Table 2: The bounds on the mass parameters, $\tan\beta$, and α_s of the MSSM under the extra constraints imposed by cold dark matter (CDM) and mixed dark matter (MDM) scenarios, for $M_t = 170$. The last column (MDM/CDM + FT) gives the upper bound when either the CDM or MDM scenario is assumed and the requirement of low fine-tuning ($f \leq 50$) is additionally imposed. Uncertainties in the values are discussed in text and in caption of 1.

While neither of these DM scenarios is free from problems, it is nevertheless interesting to point out which regions of the parameter space of the CMSSM they select. This is illustrated in Fig. 6 and in Table 2. We see in Fig. 6 that requiring either (5) or (6) results in selecting only relatively narrow bands in the $(m_{1/2}, m_0)$ plane. Their shape and location vary with other parameters but typically correspond to both $m_{1/2}$ and m_0 in the range of a few hundred GeV, independent of the choice of A_0 and $\mathrm{sgn}\,\mu_0$. The resulting mass ranges are presented in Table 2 for $M_t = 170\,\mathrm{GeV}$. They should be compared with those listed in Table 1 for the same M_t to appreciate how much more limited the mass ranges become after the MDM/CDM assumption is made. It is clear that, with the exception of the light Higgs h^0, the mass spectra consistent with either CDM or MDM are typically beyond the current experimental reach. Conversely, a discovery of a slepton at LEP II, or a squark (other than the stop) or gluino at the Tevatron well below the limits given in Table 2, while providing unquestionable evidence for supersymmetry, would at the same time indicate clear deficiency in the neutralino relic abundance [25] below the expected ranges of (5) or (6), in the scenario with b–τ unification and small $\tan\beta$.

Finally, as we have noted previously, the tiny region $m_0 \gg m_{1/2} \simeq m_Z$, corresponding to the Z- and h^0-pole annihilation of the LSPs, is the region favored by the non-observation of proton decay in $SU(5)$-type models with minimal Higgs sectors [14].

5 Conclusions

The predictability of the CMSSM becomes significantly enhanced by an additional assumption of b–τ unification at least in the region of small $\tan\beta$ which we have studied here. Our main conclusions can be summarized as follows:

1. The parameter space of the CMSSM is now completely limited both from below (by experimental constraints) and from above ($m_0 \lesssim 500\,\text{GeV}$ and $m_{1/2} \lesssim 1\,\text{TeV}$) by robust cosmological constraints, without having to invoke the a fine-tuning constraint. This is a specific case of a more general property of the CMSSM: for either small $\tan\beta$ (close to one) or for large $M_t \gtrsim 170\,\text{GeV}$ the parameter space is *always* (*i.e.*, for any choice of other parameters) constrained from above broadly within the 1 TeV mass range. Both of these cases are selected by the requirement of low $\tan\beta$ b–τ unification.

2. The resulting sparticle mass spectra are highly constrained and correlated. All the colored sparticles (except for the lighter stop) are typically very heavy, and so are the heavier Higgs bosons (A^0, H^0, $H^\pm$). The lightest neutralino is the LSP, and it is invariably predominantly bino-like. Also, $m_{\chi_1^\pm} \simeq m_{\chi_2^0} \simeq 2m_\chi$. The resulting mass ranges, with and without imposing the additional fine-tuning constraint, have been listed in Table 1. It is clear that one can make a number of predictions which can falsify the specific scenario considered here. It would be ruled out, for example, if M_t came out to be about 170 GeV and the gluino or a squark (other than a stop) were discovered at Fermilab well below 200 GeV; similarly, the sleptons cannot be much lighter than 65 GeV.

3. Additional stringent constraints are provided by requiring the neutralino LSP to provide most of presumed dark matter in the flat universe, as we can see from Table 2. Again, we find that the lower bound on the slepton masses (including the stau) are beyond the reach of LEP II, while the squarks and the gluino could possibly be discovered with the upgraded Tevatron in a limited region of parameter space. Thus, finding such sparticles with masses well below the ranges given in Table 1 would provide us with important information about the status of the neutralino as the dominant component of DM in the universe.

4. The predictions for $\text{BR}(b \to s\gamma)$ in this scenario fall almost completely within the range favored recently by CLEO, and near to the SM prediction. Furthermore, for solutions with light spectra a sharp dependence arises in the prediction of $\text{BR}(b \to s\gamma)$ on $\text{sgn}\,\mu_0$. However, both theoretical and experimental uncertainties must be reduced before one will be able to constrain a large portion of the parameter space or determine $\text{sgn}\,\mu_0$ through this signal.

5. In this restrictive scenario with imposed radiative electroweak symmetry breaking an additional correlation between μ and $m_{1/2}$ arises (see Eqs. (3)–(4)) which may be helpful in a limited way in various phenomenological studies.

Finally, which of the properties of the CMSSM sparticle spectra and predictions are specific to the b–τ unification assumption? Essentially, the crucial ingredient is the requirement that $\tan\beta$ be close to one. In this case the tree-level contribution to m_{h^0} is negligible and

h^0 is light enough to exclude large regions of the parameter space for smaller M_t. Also, the neutralino LSP pair-annihilation is genuinely somewhat suppressed for $\tan\beta \simeq 1$ leading to too much relic abundance ($\Omega_\chi h_0^2 > 1$) for $m_{1/2}$ and m_0 smaller than in the general case. Allowing for larger $\tan\beta$ relaxes both lower and upper limits on both $m_{1/2}$ and m_0 [2] and thus on the sparticle and Higgs masses. Clearly, the sparticle mass spectroscopy of the next generation of colliders will teach us a great deal about our theoretical expectations, in particular on the question of b–τ unification.

6 Acknowledgements

This work was supported in part by the U.S. Department of Energy and the Texas National Research Laboratory Commission.

References

[1] P. Langacker, in the *Proceedings of the PASCOS-90 Symposium*, eds. P. Nath and S. Reucroft (World Scientific, Singapore, 1990); P. Langacker and M.-X. Luo, Phys. Rev. **D44** (1991) 817; J. Ellis, S. Kelley, and D.V. Nanopoulos, Phys. Lett. **B260** (1991) 131; U. Amaldi, W. de Boer, and H. Fürstenau, Phys. Lett. **B260** (1991) 447; F. Anselmo, L. Cifarelli, A. Peterman, and A. Zichichi, Nuovo Cim. **104A** (1991) 1817, and Nuovo Cim. **105A** (1992) 581.

[2] G.L. Kane, C. Kolda, L. Roszkowski, and J. Wells, Michigan preprint UM-TH-93-24 (October 1993), Phys. Rev. **D,** *in press.*

[3] V. Barger, M.S. Berger, P. Ohmann, and R.J.N. Phillips, Phys. Lett. **B314** (1993) 351.

[4] M. Carena, S. Pokorski, and C. Wagner, Nucl. Phys. **B406** (1993) 59.

[5] P. Langacker and N. Polonsky, Phys. Rev. **D49** (1994) 1454.

[6] H. Arason, D. Castaño, B. Keszthelyi, S. Mikaelian, E. Piard, P. Ramond, and B. Wright, Phys. Rev. Lett. **67** (1991) 2933.

[7] H. Arason, D. J. Castaño, B. Keszthelyi, S. Mikaelian, E. J. Piard, P. Ramond, and B. D. Wright, Phys. Rev. **D46** (1992) 3945; S. Titard and F.J. Ynduráin, Michigan preprint UM-TH-93-25 (September 1993).

[8] The LEP Collaborations ALEPH, DELPHI, L3, OPAL, and The LEP Electroweak Working Group, CERN/PPE/93-157 (August 1993).

[9] B. Ananthanarayan, G. Lazarides, and Q. Shafi, Phys. Lett. **B300** (1993) 245; B. Ananthanarayan and Q. Shafi, Bartol preprint BA-93-25 (June 1993, revised November 1993).

[10] L. Hall, R. Rattazzi, and U. Sarid, LBL preprint LBL-33997 (June 1993, revised February 1994).

[11] M. Carena, M. Olechowski, S. Pokorski, and C. Wagner, CERN preprint CERN-TH.7163/94 (February 1994).

[12] A. Nelson and L. Randall, Phys. Lett. **B316** (1993) 516.

[13] P. Langacker and N. Polonsky, Pennsylvania preprint UPR–0594T (February 1994).

[14] R. Arnowitt and P. Nath, Phys. Lett. **B287** (1992) 89; Phys. Rev. Lett. **69** (1992) 725; Phys. Lett. **B299** (1993) 58.

[15] K.S. Babu and S.M. Barr, Phys. Rev. **D48** (1993) 5354; Bartol preprint BA-94-04 (1994).

[16] B. Ananthanarayan, K.S. Babu, and Q. Shafi, Bartol preprint BA-94-02 (January 1994).

[17] H. Baer, M. Drees, C. Kao, M. Nojiri, and X. Tata, Florida State preprint FSU-HEP 940311 (March 1994).

[18] R. Hempfling and A. Hoang, DESY preprint DESY-93-162 (November 1993); but see also J. Kodaira, Y. Yasui, and K. Sasaki, Hiroshima preprint HUPD-9316 (November 1993).

[19] A. Brignole, J. Ellis, J.F. Gunion, M. Guzzo, F. Olness, G. Ridolfi, L. Roszkowski, and F. Zwirner, in the *Proceeding of the Workshop "e^+e^- Collisions at 500* GeV*: The Physics Potential"*, ed. P. Zerwas, DESY preprint 92-123A (August 1992).

[20] Z. Kunszt and F. Zwirner, Nucl. Phys. **B385** (1992) 3; V. Barger, M.S. Berger, A. Stange, and R.J.N. Phillips, Phys. Rev. **D45** (1992) 4128; J.F. Gunion and L.H. Orr, Phys. Rev. **D46** (1992) 2052; H. Baer, M. Bisset, D. Dicus, C. Kao, X. Tata, Phys. Rev. **D47** (1993) 1062; H. Baer, M. Bisset, C. Kao, X. Tata, Florida State preprint FSU-HEP-940204 (February 1994).

[21] J. Gunion and H. Pois, U.C.-Davis preprint UCD-94-1 (January 1994).

[22] S. Bertolini, F. Borzumati, A. Masiero, and G. Ridolfi, Nucl. Phys. **B353** (1991) 591; R. Barbieri and G. Giudice, Phys. Lett. **B309** (1993) 86. See also F. Borzumati, DESY preprint DESY-93-090 (August 1993).

[23] M. Carena, M. Olechowski, S. Pokorski, and C. Wagner, CERN preprint CERN-TH.7060/93 (October 1993).

[24] S. Kelley, J.L. Lopez, D.V. Nanopoulos, H. Pois, and K. Yuan, Nucl. Phys. **B398** (1993) 3.

[25] L. Roszkowski, Phys. Lett. **B278** (1992) 147.

This figure "fig1-1.png" is available in "png" format from:

http://arXiv.org/ps/hep-ph/9404253v1

This figure "fig2-1.png" is available in "png" format from:

http://arXiv.org/ps/hep-ph/9404253v1

This figure "fig1-2.png" is available in "png" format from:

http://arXiv.org/ps/hep-ph/9404253v1

This figure "fig2-2.png" is available in "png" format from:

http://arXiv.org/ps/hep-ph/9404253v1

This figure "fig1-3.png" is available in "png" format from:

http://arXiv.org/ps/hep-ph/9404253v1

This figure "fig1-4.png" is available in "png" format from:

http://arXiv.org/ps/hep-ph/9404253v1